

## Magnetic Field Line Tracing Calculations for Conceptual PFC Design in the National Compact Stellarator Experiment

R. Maingi<sup>a</sup>, T. Kaiser<sup>b</sup>, D.N. Hill<sup>b</sup>, J.F. Lyon<sup>a</sup>, D. Monticello<sup>c</sup>, M.C. Zarnstorff<sup>c</sup>

<sup>a</sup> Oak Ridge National Laboratory

<sup>b</sup> Lawrence Livermore National Laboratory

<sup>c</sup> Princeton Plasma Physics Laboratory

The National Compact Stellarator Experiment (NCSX) is a three-field period compact stellarator presently in the construction phase at Princeton, NJ. The design parameters of the device are major radius  $R=1.4\text{m}$ , average minor radius  $\langle a \rangle = 0.32\text{m}$ ,  $1.2 \leq \text{toroidal field } (B_t) \leq 1.7 \text{ T}$ , and auxiliary input power up to 12 MW with neutral beams and radio-frequency heating. The NCSX average aspect ratio  $\langle R/a \rangle$  of 4.4 lies well below present stellarator experiments and designs, enabling the investigation of high  $\beta$  physics in a compact stellarator geometry. Also the NCSX design choice for a quasi-axisymmetric configuration aims toward the achievement of tokamak-like transport. In this paper, we report on the magnetic field line tracing calculations used to evaluate conceptual plasma facing component (PFC) designs.

In contrast to tokamaks, continuous target plates are not required to intercept the

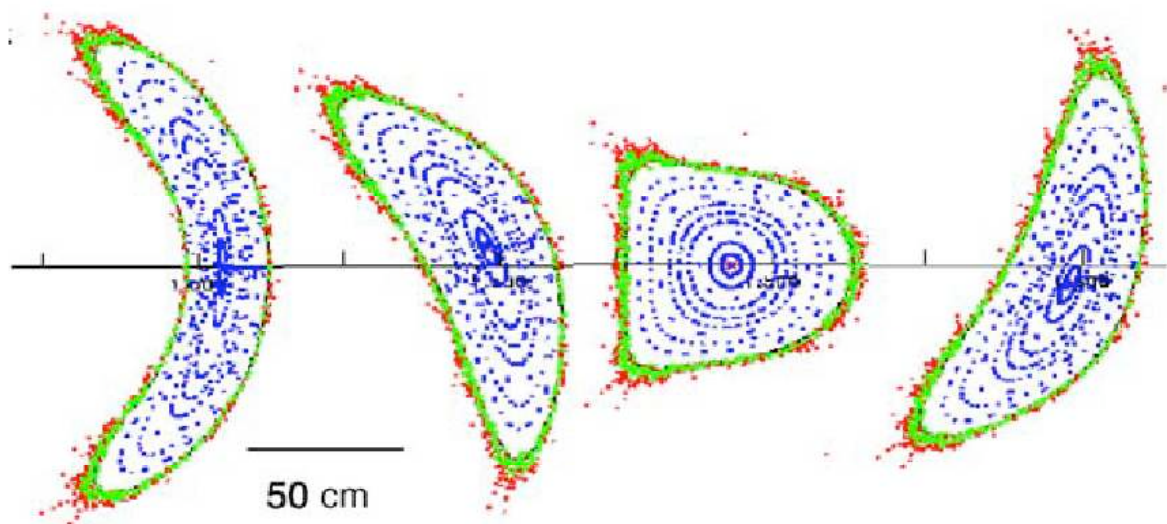


Fig. 1 – Poincaré plots from field lines traced from a full-current, high beta equilibrium<sup>1</sup>: (a)  $\phi=0$ , (b)  $\phi=\pi/6$ , (c)  $\phi=\pi/3$ , and (d)  $\phi=\pi/2$ . The red (green) field lines were launched from the inner (outer) midplane.

majority of the heat flux in stellarators, owing to the nature of the 3-D magnetic field footprint. The divertor plate design investigated in this study covers approximately one

half of the toroidal extent in each period. Typical Poincaré plots in Figure 1 illustrate the plasma cross-section at several toroidal angles for a computed NCSX high-beta equilibrium. The plates used for these calculations are centered in each period about the elongated cross-section shown in Figure 1a, extending to  $\pm \pi/6$  in each direction.

Two methods for tracing the edge field line topology were used in this study. The first entails use of the VMEC/MFBE-2001 packages<sup>1,4</sup>, whereas the second entails use of the PIES code<sup>5</sup> with a post-processor by Michael Drevlak; the same field line integration routine was used to evaluate the equilibria for this comparison<sup>6</sup>. Both inputs were generated based on the  $\beta=4\%$  equilibrium computed from the final NCSX coil set. We first compare these two methods for a specific plate geometry, and conclude with a comparison of the strike characteristics for two different target plate poloidal lengths using the latter method.

The details of the magnetic topology differ somewhat when computed with VMEC/MFBE as compared with an iterated PIES solution. The presence of islands in the PIES solution effectively reduces the radius of the last closed magnetic surface (LCMS) by several cm. The impact of this difference was minimized by following field lines in both equilibria inside of the PIES LCMS. Nonetheless, the difference in the edge topology does translate to a difference in field line terminations, as discussed below.

To quantify the impact of the VMEC/MFBE and PIES equilibrium differences on target footprints, 1000 field lines were launched from the  $\phi=0^0$  toroidal angle location in each equilibrium. Target plates of 10 cm poloidal length with a toroidal extent of  $\pm \pi/6$  were used. The projections of these plates are shown for several cross-sections in Figure 2. Note that the area behind the target plates separated from the vessel wall is indicated as the divertor shadow region. Particle diffusion was simulated with a field line cross-field diffusion rate of  $1 \text{ m}^2/\text{s}$ . Field lines were followed until they terminated at the divertor target, in the divertor shadow region, or at the wall. The field line tracing was also terminated if the field line length exceeded 1000 m, because that length would be sufficient to radiate away the parallel heat flux prior to reaching a surface.

Table 1 shows that the field line termination statistics for the VMEC and PIES equilibria are generally comparable: most of the field lines terminate at the divertor for each case, and none of the field lines make it to the wall. There are statistically significant differences: more field lines terminate in the divertor shadow region in the PIES equilibrium. Of the field lines intersecting the divertor targets, the PIES equilibrium shows

a 4:1 split between outboard divertor and inboard divertor terminations, whereas the VMEC/MFBE equilibrium shows no terminations at the inboard targets at all. In addition, many more field lines reach the upper limit of 1000m in the VMEC equilibrium. More work is required to understand these differences.

Table I also compares the effectiveness of 10cm long or 15cm long plates in the PIES equilibrium. The 10cm plates were elongated by 2.5cm on each side to construct the 15cm plates. The longer plates successfully catch more field lines than the shorter plates, by preventing field lines from entering the shadow region. Additionally, appropriately designed target plates could be easily inserted to prevent those field lines in the shadow region from terminating at the wall behind the divertor targets.

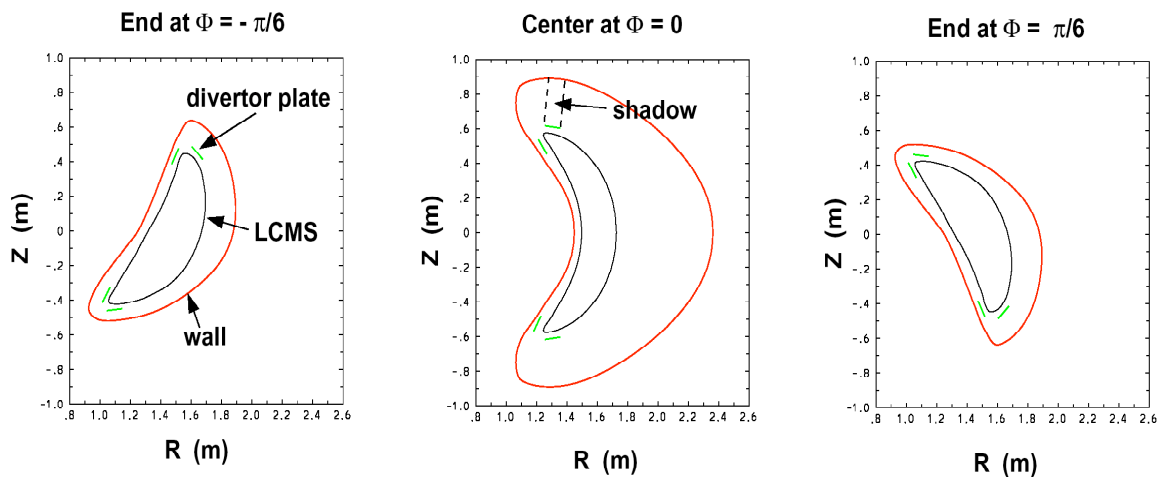


Fig. 2 – Poloidal cross-section at several toroidal angles with location of 10cm long upper and lower divertor plates.

In summary, we find that divertor effectiveness is comparable with the VMEC/MFBE equilibrium and the PIES equilibrium for the 10cm long target plate considered. We also find that increasing the poloidal length of the target plate from 10cm to 15cm leads to a marginal improvement in the efficiency as measured by the fraction of field lines impinging on the targets. Detailed sensitivity studies are required for the actual NCSX target plate design, including further variation of the poloidal and toroidal lengths, variation of the plasma/wall gap, variation of the iota profile and the beta in the equilibrium itself. Furthermore a comparison of measured heat and particle flux patterns with predictions from these codes applied to existing or previous stellarators would lend additional credibility for the use of these codes in target design.

Table 1 – Comparison of field line terminations with the VMEC/MFBE and PIES equilibria

Field line termination	VMEC/MFBE (10 cm)	PIES (10 cm)	PIES (15 cm)
Hit any divertor	84	70	82
Hit lower outboard divertor	48	30	38
Hit upper outboard divertor	36	25	23
Hit lower inboard divertor	0	9	10
Hit upper inboard divertor	0	6	11
Entered Divertor shadow region	8	29	17
Length > 1000m (stopped following)	8	1	1
Hit vacuum vessel wall	0	0	0

### Acknowledgements

We acknowledge discussions with Arthur Grossman (University of California at San Diego). This research was supported by US D.O.E. contracts by the U.S. Dept. of Energy under contracts DE-AC05-00OR22725, W-7405-ENG-48, and DE-AC02-76CH03073.

### References

- <sup>1</sup> P. K. Mioduszewski, J. Nucl. Materials **313-316**, 1304 (2003).
- <sup>2</sup> S. P. Hirshman, Comput. Phys. Comm. **43**, 143 (1986).
- <sup>3</sup> E. Strumberger, Nuclear Fusion **37**, 19 (1997).
- <sup>4</sup> A. Grossman, J. Nucl. Materials **337-339**, 400 (2005).
- <sup>5</sup> A. H. Reiman, Computer Physics Comm. **43**, 157 (1986).
- <sup>6</sup> T. B. Kaiser, Bull. Am. Phys. Soc. **49**, 313 (2004).